

DOI: 10.1093/femsec/fiad081

Advance access publication date: 18 July 2023

Research Article

# Microbiome convergence and deterministic community assembly along successional biocrust gradients on potash salt heaps

Juliette A. Ohan <sup>1,2</sup>, Roberto Siani<sup>1,2</sup>, Julia K. Kurth <sup>1,2</sup>, Veronika Sommer<sup>3,4</sup>, Karin Glaser<sup>3</sup>, Ulf Karsten<sup>3</sup>, Michael Schloter<sup>1,2</sup>, Stefanie Schulz<sup>1,\*</sup>

- <sup>1</sup>Research Unit for Comparative Microbiome Analysis, Helmholtz Center Munich, Research Center for Environmental Health, Ingolstädter Landstraße 1, 85764 Neuherberg, Germany
- <sup>2</sup>Chair of Environmental Microbiology, Department of Life Science Systems, School of Life Sciences, Technical University Munich, Alte Akademie 8, 85354 Freising, Germany
- <sup>3</sup>Institute of Biological Sciences, Applied Ecology and Phycology, University of Rostock, Albert-Einstein-Strasse 3, 18051 Rostock, Germany
- <sup>4</sup>upi UmweltProjekt Ingenieurgesellschaft mbH, Breite Straße 30, 39576 Stendal, Germany
- \*Corresponding author. Research Unit for Comparative Microbiome Analysis, Helmholtz Center Munich, Research Center for Environmental Health, Ingolstädter Landstraße 1, 85764 Neuherberg, Germany. Tel/Fax: +49 (0) 89-3187-3054; E-mail: stefanie.schulz@helmholtz-muenchen.de

  Editor: [Angela Sessitsch]

#### **Abstract**

Potash mining, typically performed for agricultural fertilizer production, can create piles of residual salt waste that are ecologically detrimental and difficult to revegetate. Biological soil crusts (biocrusts) have been found growing on and around these heaps, suggesting resilience to the hypersaline environment. We set out to understand the community dynamics of biocrust formation by examining two successionary salinity gradients at historical mining sites using a high throughput amplicon sequencing. Bare heaps were distinct, with little overlap between sites, and were characterized by high salinity, low nutrient availability, and specialized, low diversity microbial communities, dominated by Halobacteria, Chloroflexia, and Deinococci. 'Initial' stages of biocrust development were dominated by site-specific Cyanobacteria, with significant overlap between sites. Established biocrusts were the most diverse, with large proportions of Alphaproteobacteria, Anaerolineae, and Planctomycetacia. Along the salinity gradient at both sites, salinity decreased, pH decreased, and nutrients and Chlorophyll a increased. Microbiomes between sites converged during succession and community assembly process analysis revealed biocrusts at both sites were dominated by deterministic, niche-based processes; indicating a high degree of phylogenetic turnover. We posit early cyanobacterial colonization is essential for biocrust initiation, and facilitates later establishment of plant and other higher-level biota.

Keywords: bacterial diversity, biocrust, Cyanobacteria, metabarcoding, potash

# **Abbreviations**

OD: Oedesse WT: Wietze Chl  $\alpha$ : Chlorophyll a  $\beta$ -NTI: Nearest Taxon Index

# Introduction

In ecology, succession is a fundamental concept, which explains how natural communities can change and replace one another over time, particularly after disturbance (Cowles 1899). The processes that shape these changes in community assembly can be categorized as stochastic (random) or deterministic (directed); whereby stochastic processes include random births/deaths, probabilistic dispersal, and unpredictable disturbances; and deterministic processes include more consistent abiotic drivers ('environmental selection'), and positive/negative species interactions (Chase and Myers 2011). Recent work has shown that like plants, microbial communities are similarly subject to succession (Fierer et al. 2010). However, microbial succession is better opera-

tionally classified based on environment rather than classic 'primary' and 'secondary' phases in classical ecology. This is due to the widespread distribution and diversity of microbes virtually everywhere on the planet. Changes in environmental conditions affect microbial succession, and subsequently influence competition, symbioses, and functional redundancy. Further, the changes in species distribution of the community also modify the environment itself, leading to fluctuations in nutrient cycling and facilitating new microbial interactions.

Thus, soils are complex systems, whose species composition can vary greatly with abiotic factors, location, and over spatial and temporal scales (Averill et al. 2021). Accordingly, soil microbial communities have been found to be largely driven by deterministic processes (Stegen et al. 2012, 2013, Wang et al. 2013, Lee et al. 2018, Liu et al. 2021), with abiotic variables such as pH known to act as modulators between stochastic and deterministic processes (Tripathi et al. 2018).

Biological soil crusts, or 'biocrusts', are multispecies communities that act as ecological engineers and cover more than 12% of the Earth's surface, across many biomes. Biocrusts have been well-studied for decades in desert drylands (Belnap et al. 2001),

and more recently in mesic habitats (Gall et al. 2022). They host phototrophs such as algae, Cyanobacteria, lichens, and mosses, which exchange carbon (C) with heterotrophs such as bacteria, archaea, and fungi. In turn, the heterotrophs, and some clades of nitrogen (N)-fixing Cyanobacteria, provide N from organic sources and other micronutrients. Together, they aggregate mineral soil particles into a stable carpet-like 'crust' at the top few millimeters of the soil surface by producing cementing exopolysaccharides (EPS), which prevent soil erosion (Zhang et al. 2006, Chamizo et al. 2017, Cania et al. 2020). Such biocrusts improve soil qualities by increasing water-holding capacity (Chamizo et al. 2016, Gypser et al. 2016, Sun et al. 2021), decreasing infiltration into the underlying water table (Xiao et al. 2019), increasing nutrient availability to plants (Thiet et al. 2005, Belnap 2011, Su et al. 2011), and regulating microclimates (Belnap 2006). Additionally, biocrusts provide niches and microenvironments that are receptive to more diverse microbial colonization and, therefore, provide the opportunity for biological interactions including specific symbioses. However, as of yet, it is unclear if stochastic or deterministic processes dominate in shaping their microbial community structure.

Potash salt heaps are byproducts of industrial mining that are highly saline and resistant to plant growth. We identified biocrusts developing on and around two historical potash tailings sites across temperate regions in Germany (Sommer et al. 2020a, b, Pushkareva et al. 2021). Recent work found the phototrophic communities of these biocrusts transitioned from green algae to Cyanobacteria dominated upon succession, with filamentous taxa found throughout (Sommer et al. 2020a).

We propose that: (i) biocrust development is a deterministic process, during which microbial habitat conditions are improved, and thus promote more diverse microbial communities. In contrast, bare heaps are more stochastically colonized and host site-specific independent extremophiles. (ii) Consequently, microbial community composition will converge between sites as biocrusts develop, because biocrusts promote bacteria with similar functional potential and, therefore, similar phylogenetic

To test these hypotheses, we explored changes in abiotic characteristics and prokaryotic community assembly in biocrusts along salinity gradients on potash tailings piles at two different locations. We used a metabarcoding approach to assess bacterial community structure based on extracted DNA and 16S rRNA gene amplicon sequencing in combination with qPCR measurements for absolute quantification of bacteria along both transects.

# Materials and methods Site description and sample collection

Soil samples were taken from two potash tailings piles residuals in Lower Saxony, Germany in May of 2019. We surveyed microbial succession along these transects, which display a salinity gradient along the slopes. The first site, Klein Oedesse ('OD'; 52.384009 N, 10.220794 E), was mined between 1913 and 1925, with mean annual temperature (MAT) and mean annual precipitation (MAP) of 9.9°C and 617.9 mm, respectively (Deutscher Wetterdienst 2023a, b; 1991–2019). It is located in a nature reserve, adjacent to a shallow, salty pond in a woodland tract. The OD sampling area consisted of one tailings pile approximately 2 m in height, covering an area of 15 m  $\times$  20 m. The salty pond and its shore are dominated by halophytes such as Atriplex longipes, Glaux maritima, Plantago maritima, Sueda maritima, and Trifolium fragiferum, as well as the brine shrimp Artemia salina (Garve and Garve 2000).

The second site, Wietze ('WT'; 52.643704 N, 9.863592 E), was mined from 1908 to 1923, with MAT and MAP of 10°C and 680 mm, respectively (Deutscher Wetterdienst 2023a, b; 1991-2019). The WT is located in an unprotected, more residential area, with an elongated section with several potash tailings. These residues follow a north to south gradient of older to younger material, with an average height of 0.8 m and a total area of 30 m  $\times$  150 m. These residue tailings include both bare (higher salinity) and naturally revegetated (lower salinity) dumps. Here, the halophytes Gypsophila scoronerifolia and Hymenolobus procumbens have been reported (Garve and Garve 2000).

The residue material of both sites was quantitatively dominated by sulfate, followed by calcium and sodium ions, leading to electrical conductivity (EC) values of 143 to 194 mS cm<sup>-1</sup>, and pH values between 8.1 and 8.4. For more details, see Sommer et al. (2020a). We defined transects along salinity gradients at each site, starting from bare heap surface ('heap'), to an intermediate biocrust development stage ('initial'), to established biocrusts ('biocrust'; Fig. 1). The distances between the successional stages spanned 0, 2, and 4.5 m in the OD; and 0, 3.5, and 6.5 m in the WT. A total of three biological replicates along the transects were sampled at each site, resulting in 18 samples (two sites, three stages, and three replicates). All samples were taken using large Petri dishes (90 mm), closed with parafilm, and stored in the dark at 4°C. In the lab, the upper 2 mm was extracted using a sterile razor blade. Samples were split in two parts, with one frozen at -20°C for molecular analyses, and the other stored at 4°C for abiotic analysis.

#### Soil characterization

EC was measured as described in Sommer et al. (2020a). Briefly, 10 g air-dried soil (< 2 mm) was mixed with 50 ml deionized water ( $< 5 \mu S cm^{-1}$ ). After shaking for 1 h. followed by 30 min of sedimentation, the EC of the supernatant was measured with an EC meter (Seven MultiTM, Mettler Toledo, Schwarzenbach/Germany, in Lab 731 probe). For pH, dissolved organic carbon (DOC), and total dissolved nitrogen (TDN) soils were extracted with 1:4 (w/v) 0.01 M CaCl2. DOC and TDN were measured using a continuousflow photometric analyzer (CFA-SAN Plus; Skalar Analytik, Germany), as described in Balázs et al. (2021).

To quantify Chlorophyll  $\alpha$  (Chl a), samples were extracted twice as follows: First, 3 ml of 96% EtOH and about 0.3-0.5 g of MgCO<sub>3</sub> were added to 1.3-8.5 mg of sample material, incubated for 5 min in a 78°C water bath, followed by manual shaking and vortexing. Then samples were placed on ice for 10 min and centrifuged (4850  $\times$  q, 5 min, 5°C). After the extractions, absorbance of the supernatant was measured at 750, 696, 665, 649, and 632 nm in 1 cm glass cuvettes using a spectrophotometer (UV-2401 PC, Shimadzu, Kyoto, Japan). Chl a content was calculated as in Ritchie (2008) and normalized to sample material dry weight. Each sample was extracted twice (and the values summed) in order to fully quantify total Chl a.

#### **DNA** extraction

DNA was extracted from 0.4 g soil with Lysing Matrix E bead beating tubes (MP Biomedicals, USA) using the Precellys 24 tissue homogenizer (Bertin Instruments, France) and phenol:chloroform:isoamyl alcohol 25:24:1 (Sigma-Aldrich, USA) following a previously described phenol chloroform technique (Töwe et al. 2011). Negative extraction controls were generated using the same bead beating tubes without soil. DNA size and quality was verified by electrophoresis in 1% (w/v) agarose gel, checked for

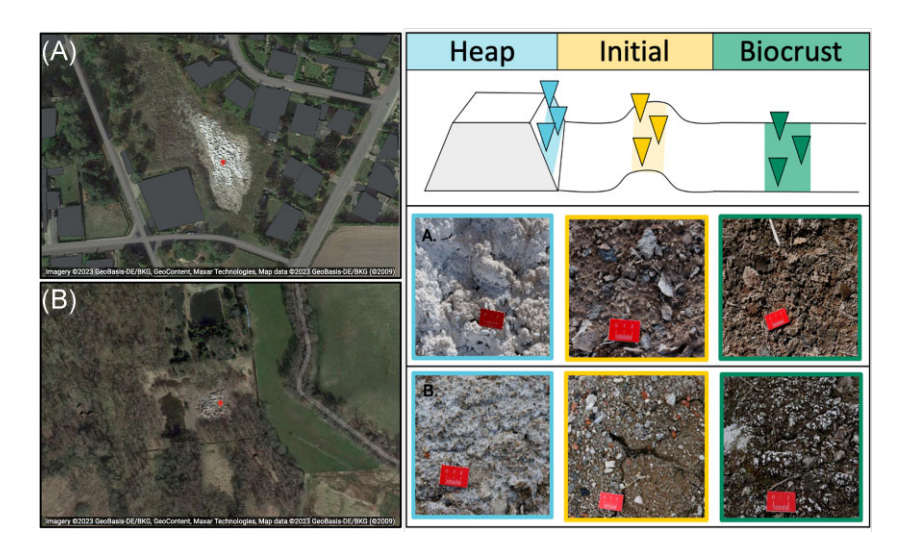


Figure 1. Sampling scheme of the salt heap gradients. Three biological replicates were taken from two potash tailings pile areas; Wietze 'WT' (A) and Oedesse 'OD' (B). Shown are the heap (blue), initial (yellow), and established biocrust (green). Red scale bar = 2 cm. Satellite images obtained from Google Earth/Maxar Technologies under fair use copyright.

purity using a NanoDrop 1000 spectrophotometer (ThermoFisher Scientific, MA, USA), and quantified using the dsDNA HS and ds-DNA BR Assay kits with a Qubit® 4.0 (ThermoFisher Scientific) Fluorometer according to manufacturer's instructions.

## Quantitative real time PCR (qPCR)

Absolute abundances of the 16S rRNA genes for bacteria and archaea were determined by qPCR using FP 16S rRNA 5'-GGTAGTCYAYGCMSTAAACG-3' and RP 16S rRNA 5'-GACARCCATGCASCACCTG-3', (Bach et al. 2002) and sAF(i) (5'-CCTAYGGGGCGCAGCAG-3', Nicol et al. 2003) and 958r (5'-YCCGGCGTTGAMTCCAATT-3', Bano et al. 2004), respectively. Amplification parameters are further described in Table S4 (Supporting Information). Preliminary tests with sample dilutions from 1:8 to 1:256 determined 1:100 to be the ideal dilution in order to limit any inhibitory effects. Standards ranged from 10<sup>1</sup> to 10<sup>7</sup> for bacterial 16S rRNA and 10<sup>2</sup> to 10<sup>8</sup> for archaeal 16S rRNA. The final 25 μl PCR reaction mix consisted of 1X Power SYBR™ Green Master Mix (ThermoFisher Scientific), 0.5  $\mu$ l of 3% BSA, 2  $\mu$ l of template DNA, and 0.2 pmol  $\mu l^{-1}$  primers. No template controls used DEPC water and were processed in the same manner. R<sup>2</sup> values ranged from 0.993 to 0.998 for the bacterial 16S rRNA gene and 0.997 to 1.0 for the archaeal 16S rRNA gene. Efficiencies ranged from 81% to 99% for bacterial 16S rRNA gene and from 81% to 83% for archaeal 16S rRNA gene. Samples were quality checked using melting curve analysis and gel electrophoresis.

#### Amplicon sequencing and processing

To determine the soil's microbial community composition, and allow the best comparability with similar studies, we sequenced the widely adapted V4 hypervariable region of the 16S rRNA gene using modified Caporaso-Parada dual-barcoded 515FB-806RB primers (Apprill et al. 2015, Parada et al. 2016) from the Earth Microbiome Project. These primers have been used to explore a diverse array of environmental microbiomes, but were recently found to have the highest microbial diversity, abundance, best depth, and most coverage for archaea and bacteria, particularly in soils (Wasimuddin et al. 2020). Quality guidelines were followed as described in Schöler et al. (2017) on the Illumina Miseq platform with 2  $\times$  300 bp chemistry. The final 25  $\mu$ l PCR reaction mix consisted of 1X NEBNext High-Fidelity PCR Master Mix (New England Biolabs, MA, USA), 2.5  $\mu$ l of 3% BSA, 10 ng of template DNA, and 0.2 pmol  $\mu$ l<sup>-1</sup> primers. Cycling parameters were 98°C for 1 min; 35 cycles of 98°C for 10 s, 55°C for 30 s, 72°C for 30 s; and 72°C for 5 min. PCR products were purified using MagSi-NGSPREP Plus magnetic beads (Magtivio, NL) at a ratio of 4:5 (v/v) of beads to DNA. Negative extraction and PCR controls were amplified using DEPC water as template and sequenced alongside samples. All samples were indexed using the Illumina v2 Nextera XT Kit, and quality checked using the 5200 fragment analyzer system (Advanced Analytical, DE). Samples were diluted to 4 nM using DEPC water, combined with 10% (v/v) of 4 nM denatured PhiX viral DNA, and pooled at equimolar concentrations prior to sequencing. The high salt concentration paired with low microbial biomass resulted in the loss of one WT heap sample throughout the sample processing, as 16S rRNA amplification was not successful.

Sequenced amplicon data were processed using the QIIME2 2019.10 pipeline (Bolyen et al. 2018). Reads were demultiplexed according to barcode sequences and trimmed by removing 20 bases from the start and end of the sequences and truncating the forward reads at 240 bases and reverse at 200 bases. Only reads with less than five expected errors were preserved and denoised using the DADA2 plugin (Callahan et al. 2016). ASVs were inferred and assigned by a naive Bayesian classifier trained against the SILVA taxonomy database (v138.1) (Quast et al. 2012). Downstream processing was conducted in R (v4.1.1) (Ihaka and Gentleman 1996) and the scripts made available at https://github.com/rsiani/ohan \_biocrust\_22. QIIME2 artefacts were imported, putative contaminant sequences were removed using R package decontam 1.16 (Davis et al. 2018), as well as any nonbacterial and nonarchaeal sequences. Species count data were normalized by scaling with ranked subsampling (Beule and Karlovsky 2020). Quality control metrics and rarefaction curves are documented in Table S5 (Supporting Information) and Figure S3 (Supporting Information), respectively. Raw sequences were uploaded the NCBI sequencing read archive under Bioproject ID PRJNA934864.

## Downstream and statistical analyses

Bar plots for abiotic and qPCR values were generated using R package ggplot2 (Wickham 2011). Statistical analyses for abiotic and qPCR values were conducted in R. Data that was not normally distributed was log transformed and had normal distribution of data or residuals. Linear regressions were performed using the command lm() with predictor variables: site location ('site'), and biocrust developmental stage along the salinity gradient ('stage'). If significant differences were found, pairwise comparisons were performed using the 'Ismeans' package v. 2.30-0. EC values were analyzed using nonparametric tests. The Kruskal-Wallis ranksum test (kruskal.test) was used to test for comparisons between sample stages, and Mann-Whitney-Wilcoxon test (wilcox.text) for one-way comparisons was used to test between site locations.

Canonical correspondence analysis (CCA) plots were generated by constraining the samples with environmental variables using the 'cca' function from the R package vegan v.2.6-2 (Dixon 2003). Clustered heatmaps were generated using the R package pheatmap v.1.0.12 (Kolde and Kolde 2015), scaled by row, and ordered using the Pearson distance measure and Ward clustering algorithm. Core Venn diagrams and core heatmaps were created using the R package ampvis2 (Andersen et al. 2018) v.2.7.9, with ASVs below 0.001% of reads excluded and ASVs only found in more than 65% of samples used for analysis.

A phylogenetic tree for all taxa was inferred by performing multiple-alignment using R package DECIPHER v.2.24 (Wright et al. 2012), and using the neighbour-joining method implemented in R package phangorn v.2.8.1 (Schliep 2011). Preprocessed data were combined into a phyloseq object for further analyses (R package phyloseq v.1.40 (McMurdie and Holmes 2013). ASVs present in less than 10% of the samples were discarded. Alpha diversity metrics (Chao1, Pielou, Shannon, and Simpson) were calculated using the R package microbiome v.1.18 (Lahti and Shetty 2018).

The spatial distribution of the samples was visualized with principal coordinate analysis using weighted Unifrac distances. ASV distribution in the same space was obtained using the phyloseq function 'ordinate'. To isolate the ASVs and discriminate the different sample-groups, differentially abundant features were first selected using Kruskal-Wallis test adjusted for multiple comparisons using the Benjamini-Hochberg procedure (Benjamini and Hochberg 1995). The selected ASVs were then passed to a random forest classification algorithm using the package caret v.6.0-92 (Kuhn 2008), which was used to obtain a measure of variable importance.

# Community assembly

In order to determine the processes that affected community assembly between samples, we followed Stegen et al. (2013). All community assembly analyses were performed using the R package 'picante' v. 1.8.2. To determine the importance of phylogeny in the assembly processes, phylogenetic signal (PS) was calculated using the components produced by the CCA (Table S7, Supporting Information). K statistics for PS were less than 1.0, indicating that closely related species within the community were not conserved and did not show strong trait similarity. However, when investigated at clade level, mantel tests for PS using the R package 'iCAMP' v.1.5.12 (Ning et al. 2020) showed noncore taxa such as Archaea had high PS (data not shown). Due to large distances between sites (> 50 km), limited sample size (< 20), and agreement with other, nonphylogenetic methods, low K values did not necessarily preclude further analyses (Kamilar and Cooper 2013). When calculating  $\beta$ -NTI (Nearest Taxon Index),  $|\beta$ NTI| < 2 indicates the pairwise comparison is not driven by deterministic processes,  $\beta$ NTI < -2 indicates homogeneous selection (significantly less phylogenetic turnover than expected by chance), and  $\beta$ NTI > +2 indicates variable selection (significantly greater phylogenetic turnover than expected by chance). In total, this meant that we compared one sample against all others, for a total of 16 comparisons per sample. Values that were found not to be driven by deterministic processes ( $|\beta NTI| < 2$ ) were further interrogated using the Bray-Curtis based Raup-Crick calculation (RCbray) (Raup and Crick 1979), where  $|RC_{bray}| < 0.95$  indicates an undominated process, RC<sub>brav</sub> > +0.95 indicates dispersal limitation, and RC<sub>brav</sub> < -0.95 indicates homogenous dispersal (Chase et al. 2011). Once the assembly process was identified for each comparison, we followed Barnett et al. (2020), to determine the relative proportion of each stochastic and deterministic process for site and stage.

## Results

# Physiochemical characteristics

Physiochemical characteristics changed comparably along both transects regardless of site. Multivariate analysis determined Chl a and DOC were explanatory variables for biocrust stages at both sites (Fig. 2; Table S1, Supporting Information). From heap to biocrust stages along the transect, Chl a increased from 0.3 to 29.87  $\mu$ g g<sup>-1</sup> dry soil at the OD site, and from 0.01 to 35.24  $\mu$ g g<sup>-1</sup> dry soil at the WT site, moderately differing between sites (P = .077; Table S2, Supporting Information). However, pairwise comparisons of Chl a along the transects of both sites revealed significant differences between all stages (Table S2, Supporting Information), with each stage grouping together regardless of site (Table S3, Supporting Information). DOC similarly increased from heap to biocrust stages at the OD site from 41.29 to 92.67  $\mu g g^{-1}$ dry soil and from 45.36 to 113.96  $\mu g \; g^{-1}$  dry soil at the WT site. DOC concentrations at heap and biocrust stages significantly differed (P < .001; Table S2, Supporting Information), and biocrust stages of both sites again grouped together (Table S3, Supporting Information).

In contrast to Chl a and DOC, EC, and pH were explanatory for heaps at both sites (Fig. 2A). EC decreased along the transects from heap to biocrust stages at the OD site from 27.75 to 2.05  $\mu$ S cm<sup>-1</sup>, and from 15.32 to 1.95  $\mu S$  cm<sup>-1</sup> at the WT site. EC significantly differed between the stages of both sites (P = .003). Similarly, pH decreased along the OD transect from 8.12 to 7.6 and from 8.85 to 7.71 along the WT transect (Fig. 2B), with significant differences between sites (P < .001) and heap and biocrust stages (P < .001; Table S2, Supporting Information). Pairwise analysis of pH again grouped the biocrust stages of both sites together (Table S3, Supporting Information).

When the samples were combined for multivariate analysis, TDN was explanatory for biocrust stages (Fig. 2A). However, upon separating by site, the TDN eigenvector skewed more toward the biocrusts of the WT than the OD (Figure S1, Supporting Information). Along the OD transect, heaps and biocrusts remained at 5.56  $\mu g$  TDN  $g^{-1}$  and 5.46  $\mu g$  TDN  $g^{-1}$  dry soil, respectively, while initial stages were lower at 3.7  $\mu g g^{-1}$  dry soil. Along the WT transect, TDN increased from heap to biocrust stages from 6.2 to 21.95 µg  $g^{-1}$  dry soil, with significant differences between all stages of the WT (P < .001).

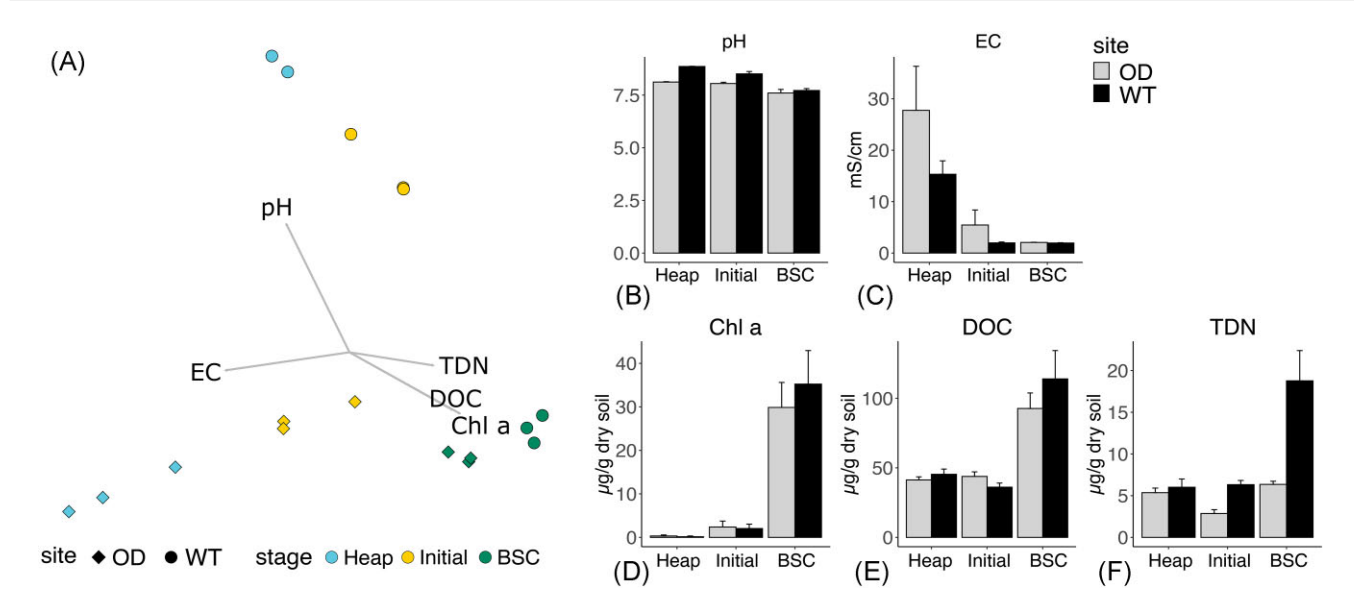


Figure 2. Abiotic properties. (A) CCA with physiochemical variables that drive variation between samples in both sites, and (B)-(F) abiotic characteristics on the biocrust (BSC) gradient: pH, EC, Chl a, DOC, and TDN. Error bars show the standard deviation for three biological replicates

# Quantification of bacterial and archaeal marker genes by qPCR

Bacterial absolute abundance as measured by gene copy numbers per  $g^{-1}$  dry soil increased along the transects of both sites. The absolute abundance of the bacterial 16S rRNA gene marker increased from  $5.01 \times 10^7$  to  $5.76 \times 10^9$  (copies  $g^{-1}$  dry soil) at the OD site and from  $3.87 \times 10^5$  to  $1.87 \times 10^{10}$  (copies  $g^{-1}$  dry soil) at the WT site (Figure S2, Supporting Information). Accordingly, bacterial absolute abundance significantly differed between heap and biocrusts (P < .001), but not by site, (Table S2, Supporting Information). Archaeal absolute abundance (16S rRNA) also increased from heap to biocrust from  $4.03 \times 10^3$  to  $8.51 \times 10^8$  (copies g<sup>-1</sup> dry soil) in the WT transect, but remained from  $10^7$  to  $10^8$  (copies  $g^{-1}$ dry soil) in all stages of the OD. Overall, archaeal absolute abundance did not significantly differ between stages or by site. However, copy numbers of the WT heap were significantly lower than all other samples (P < .001; Table S2, Supporting Information). Relative abundance values (copies ng<sup>-1</sup> DNA) showed similar trends as described above (Figure S2, Supporting Information). Pairwise analysis of both bacterial and archaeal relative abundance of 16S rRNA genes indicated similarities between samples from OD initial and OD biocrusts as well as biocrusts of both sites together.

# Microbial diversity along the successional transect

Site location and developmental stage both affected microbial alpha diversity. Shannon diversity (Fig. 3A) and richness (Fig. 3B) increased with biocrust development at both sites, but the OD was more diverse than the WT at every developmental stage. At both sites, initial stage microbial communities were more dominant than later biocrust stages, likely due to higher relative abundances of Cyanobacteria (21.7% OD, 23% WT; Fig. 3C-E). Heap microbial communities were also dominant in the WT, while in the OD, halophilic Euryarchaeota of the class Halobacteria were abundant (51.2% OD, 0.4% WT; Fig. 3C-E). The genera within this class were very diverse, and therefore, likely contributed to higher evenness (Fig. 3D), corresponding to lower dominance as compared to the WT (Fig. 3C).

When all samples were clustered on ASV level using the Pearson distance metric and Ward clustering algorithm, bacterial communities of heaps and initial stages at each site grouped together, and biocrust stages of the WT biocrusts formed a clear separate outgroup (Fig. 4A). Principle coordinate analysis (PCoA) using phylogenetically informed Unifrac distances showed samples converged from heap to biocrust (along the transects) at both sites (Fig. 4B). Heap samples grouped together by site, and were defined by halophilic and extremophilic differentially abundant taxa. The same pattern held for samples from initial stages, generally grouping together by site, except for one OD sample, which grouped closer to biocrust stages.

#### Microbial community composition

Distinct microbial assemblages marked each developmental stage independent of site. Heaps only shared 7.7% equaling 17 ASVs between both sites (Fig. 5A), of which, a large proportion were Acidimicrobiia (Actinobacteria) and Gammaproteobacteria (Figure S4A, Supporting Information). Generally, Gammaproteobacteria decreased along the transects (with declining salinity), while Alphaproteobacteria increased (Fig. 3E). Along with the abundant halophiles (Euryarchaeota) in the heaps, we found Trueperaceae of phylum Deinococcus-Thermus (1.1% OD, 9.6%, WT), Actinobacteria such as Rubrobacteriaceae (7.5% WT), and Nitriliruptoraceae (7.4% WT), and several groups of Chloroflexi such as JG30-KF-CM45 (15.7% WT; Figure S6, Supporting Information). Chloroflexi were only abundant at the WT site (20.8% heap; Fig. 3E), and decreased along that transect. When analyzed by percentage of core, the heaps at both sites shared Actinobacteria such as N-fixing Frankiales (24.1% OD, 23.1% WT; of core) and Aquipuribacter (14.9% OD, 9% WT; of core) as well as halophilic Proteobacteria Hahella (6.9% OD, 14.2% WT; of core; Figure S5A, Supporting Information).

Initial stages of the WT were defined by Cyanobacteria (Phormidiaceae), unassigned Frankiales, and extremophilic taxa (Euryoarcheota Truepera), among others (Fig. 5C). Initial stages at the OD were specifically associated with Proteobacteria Hoeflea and cosmopolitan Devosiaceae, with the latter also the only taxa to define OD biocrusts (Fig. 5C). Initial and

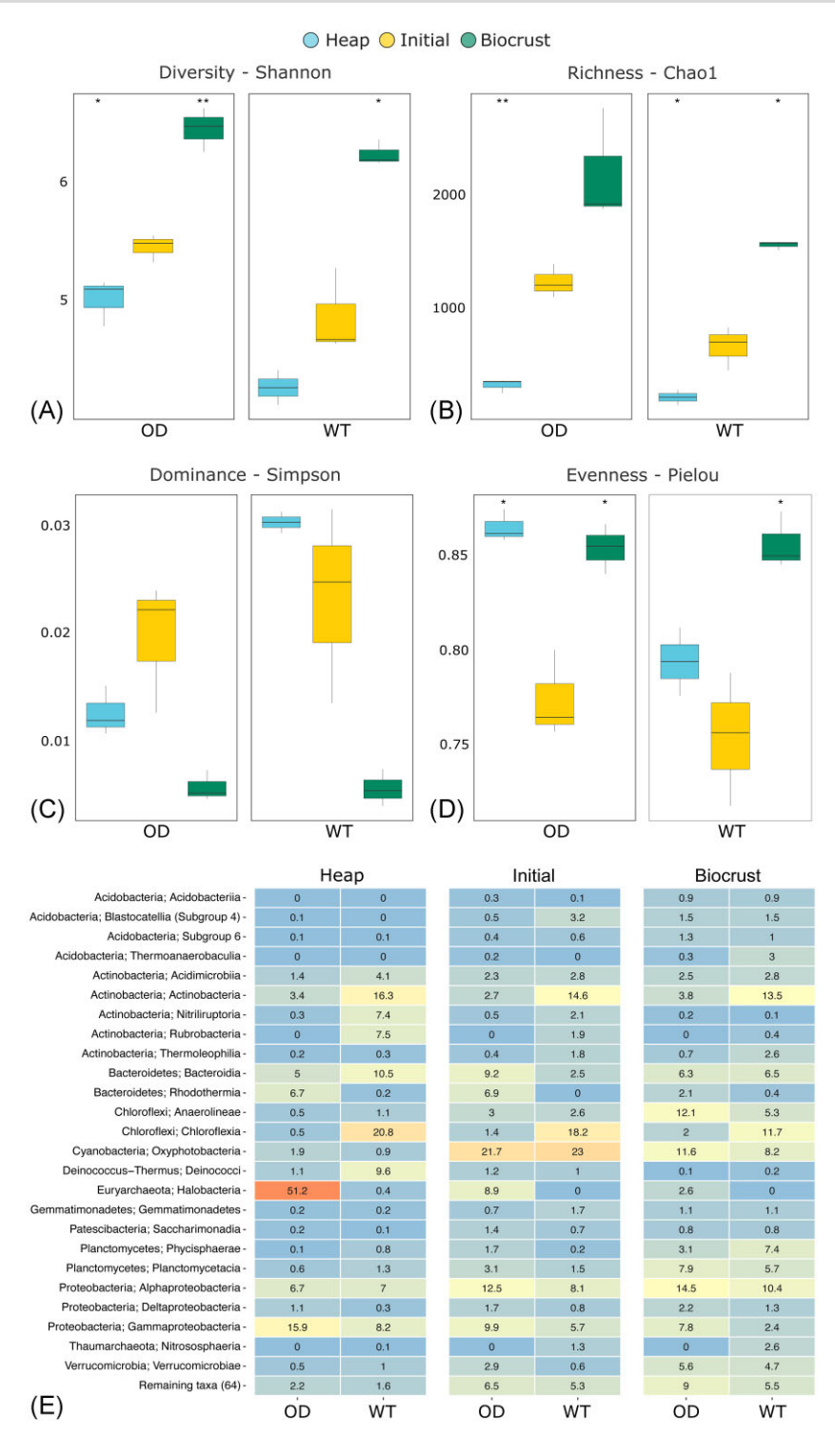


Figure 3. Diversity indices and microbial community composition. (A) Diversity by Shannon, (B) species richness by chao1, (C) dominance by Simpson, and (D) evenness by Pielou. Significance levels (P-values) \*= .05 and \*\*= .01. (E) Relative percentage of all bacterial taxa (as class ordered by phylum).

biocrust stages at the WT site were closest in vector space to Proteobacteria Noviherbaspirillum and TRA3-20 (Fig. 4B). Bacterial communities of initial stages shared 22.5% equaling 122 ASVs between sites (Fig. 5A), and were dominated by Cyanobacteria. Predictably, Oxyphotobacteria were highest in the initial stages (21.7% OD, 23% WT) and decreased in biocrust stages in relative abundance (11.6% OD, 8.2% WT; Fig. 3E). They were largely composed of Nodosilineaceae (11.3% OD, 11% WT;

Figure S6, Supporting Information). Other prominent Cyanobacteria included an unknown genus of Coleofasiculaceae (5.6%, OD initial), Phormidiaceae (7.4%, WT initial), Leptolyngbyaceae (3.9% OD biocrust), and Microcoleus PCC-7113 (2.1% WT biocrust). When analyzed by percentage of core, initial stages shared the largest proportions of Cyanobacteria Nodosilinea (40% OD, 14.9% WT; of core), Proteobacteria such as Burkholderiaceae (4.2% OD, 11.2% WT; of core), Pseudoxanthomonas (4.2% OD, 0.4% WT; of core), and

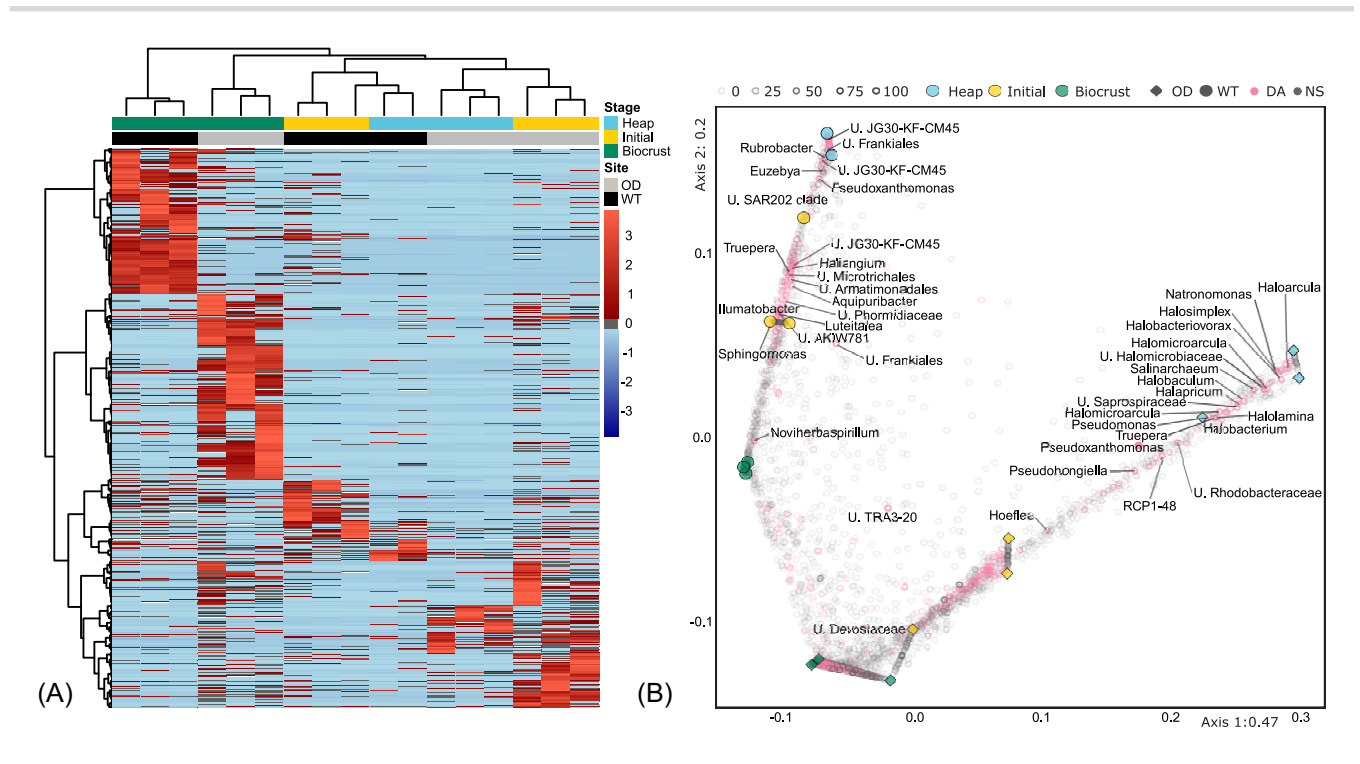


Figure 4. Grouping of samples using different metrics. (A) Relative abundance of amplicon sequence variants for all samples (ASVs), clustered using the Pearson distance measure and Ward clustering algorithm, (B) PCoA plot on weighted UniFrac distances. Predictive potential of each ASV was calculated by random forest and differential abundance across groups was determined using the Kruskal-Wallis test (variable importance was computed only on the taxa passing the KW filter and with a Benjamini-Hochberg corrected P-value lower than .05). ASVs belonging to the 100th percentile of the RF predictive potential scores are depicted in pink. Differentially abundant ASVs are labelled according to their genera.

Actinobacteria such as Aquipuribacter (2.1% OD, 12% WT; of core; Figure S3C, Supporting Information).

Biocrust stages shared 21.5% equaling 254 ASVs between sites (Fig. 5A) and hosted the highest proportions of total Planctomycetes (11.7% OD, 13.1% WT; Fig. 3E), total Acidobacteria (5.3% OD, 6.7% WT), Verrucomicrobia (5.6% OD, 4.7% WT), and Thaumarchaeota (Nitrososphaeria) (0.1%-2.6%, WT only). Biocrust stages also hosted several families in Chloroflexi such as A4b (8.8% OD, 1.2% WT), and Planctomycetes Pirellulaceae (5% OD, 2.4% WT) and WD2102 soil group (1% OD, 7% WT; Figure S6, Supporting Information). CPR group genera Saccharimonadia (Patescibacteria) were also present in small percentages in biocrusts; with an increase in parent taxon from heap to biocrust in both sites (0.2%-0.8%, OD; 0.1%-0.8%, WT; Fig. 3E). When analyzed by percentage of core, biocrust stages shared Verrucomicrobia such as Chthoniobacter (6.3% OD, 6.4% WT; of core), Actinobacteria such as Pseudonocardia (3.7% OD, 2.8% WT; of core) and Plancytomycetes (Figure S5C, Supporting Information).

# Microbial community assembly

Pairwise analysis of  $\beta$ NTI found community assembly of biocrust stages were dominated by deterministic processes ( $|\beta NTI| > 2$ ), while heap and initial site pairs were mostly stochastic ( $|\beta NTI| < 2$ ; Fig. 6A.). Most notably, variable selection ( $\beta$ NTI > 2) was the most influential pattern of phylogenetic turnover in biocrust stages at both sites (60%–73%), but was also present in lower percentages in bacterial communities of heap and initial stages (19%-36% of site pairs; Fig. 6B.). The % of site pairs dominated by homogenizing selection ( $\beta$ NTI < -2) were largely relegated to heaps (29%–36%), and decreased as biocrusts developed, but still made up of 20% of the WT biocrust site pairs while remaining low in the OD biocrust pairs (4%).

Stochastic processes were dominant in both bacterial communities from initial and heap stages. Of the stochastic processes, dispersal limitation (RC bray > 0.95) made up the highest percentage of site pairs (9%-33%), and was highest in OD initial and WT heap, respectively. Ecological drift or 'undominated' processes  $(|RC_{bray}| < 0.95)$  explained approximately 20% of both sites heap and initial site pairs. Homogenizing dispersal (RC bray < -0.95) was negligible, and only contributed to 2% of site pairs in the OD heap and WT initial communities.

#### Discussion

# Changing abiotic conditions increase niche space for generalists

Changing abiotic parameters improved conditions for bacteria along the transects. Factors attributable to biocrust establishment include photosynthetic activities (Chl a) and the associated increase of bioavailable organic carbon (DOC) (Figure S1, Supporting Information). At both sites, Chl a and DOC increased as the biocrusts developed. However, TDN remained more site-specific and was higher in the WT than the OD, possibly due to salt heap age or the protected status of the region, which could potentially influence N deposition through legal restrictions. Additionally, WT biocrusts hosted the highest concentrations of Thaumarchaeotal Nitrososphaeria a potential ammonia oxidizer (Könneke et al. 2005, Treusch et al. 2005), which might benefit from high N concentrations. Other studies found moss-dominated biocrusts contained higher amounts of organic matter than Cyanobacteria or algae-dominated biocrusts (Drahorad et al. 2021). As we also found mosses (Figure S7, Supporting Information) and chloroplast sequences in biocrusts in the WT that could be assigned to Bryum

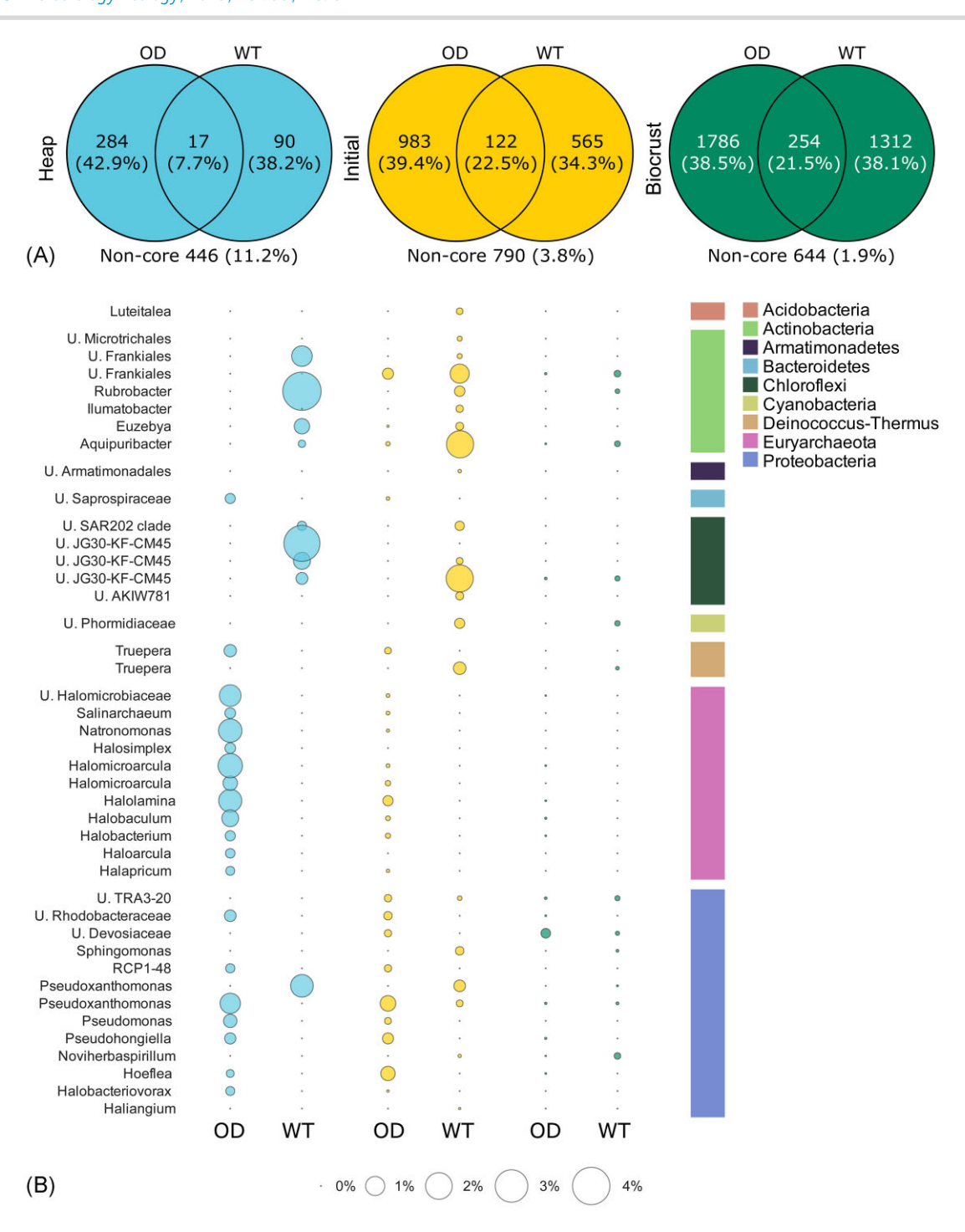


Figure 5. Microbial community composition across sites. (A) Number of ASVs and relative percentage of total reads constituted by the core microbiomes of the sample types as shared by the sites. (B) Differentially Abundant ASVs as shown in the PCoA of Fig. 4(B), sorted by phylum.

 $\it argenum$  (data not shown), this could also explain the higher levels of TDN compared to the OD.

Salinity and pH decreased along the transects. Both factors are widely known to act as drivers for community composition in soils (Fierer and Jackson 2006, Lauber et al. 2009, Rath et al. 2019). The decrease in salinity along both transects was significant, and likely played a role in the decline of extremophiles such as Rubrobacteria (Norman et al. 2017), Nitriliruptoria, thermophilic JG30-KF-CM45 (Thermomicrobia) and radiation-tolerant Deinococci (Carreto et al. 1996, Battista 1997, Rainey et al. 2005) from heaps to biocrusts. Higher salinity levels of the OD heap,

which was twice as saline as the WT heap, could have contributed to the higher abundance of halophiles in the OD. However, other factors such as initial colonization events or land management of the surrounding areas could have also contributed to different starting communities (Schöps et al. 2018, Le Provost et al. 2023). The decrease in pH was similarly strong between sites and ranged from 7.3 to 8.9, potentially driving changes in community composition, particularly as Cyanobacteria naturally prefer to colonize neutral to alkaline soils (Rossi et al. 2022). Decreases in pH have been previously observed in other arid (Riveras-Muñoz et al. 2022) and temperate biocrusts (Kurth et al. 2021), while other

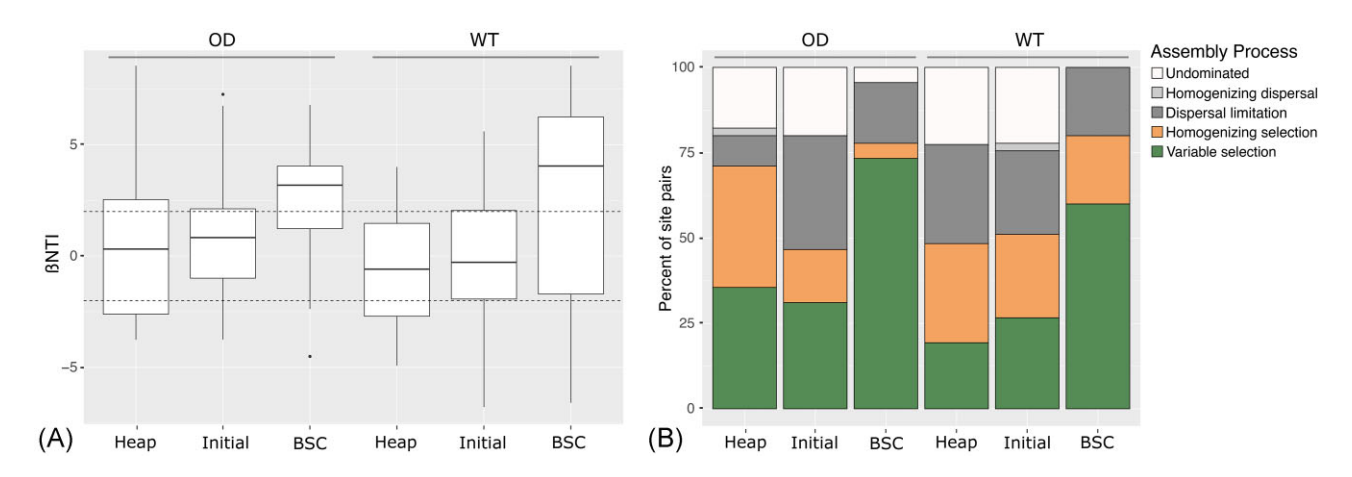


Figure 6. Community Assembly Analysis (A) Beta-NTI and (B) Community assembly processes for each stage ("BSC" = biocrust) and site. Coloured bars correspond to deterministic processes, and grey bars correspond to stochastic processes.

studies have found biocrusts can increase pH (Garcia-Pichel and Belnap 1996, Rivera-Aguilar et al. 2009) through increased microbial respiration (Chamizo et al. 2012), or algal/cyanobacterial photosynthetic activity (Glaser et al. 2022). Additionally, due to the potash heaps' high concentration of salts, microbial activity could have contributed to solubilization and subsequent release of cations and protons into the biocrust/soil matrix (Bowker et al. 2016), making compounds more bioavailable for subsequent plant or microbial uptake (Abed et al. 2019).

# Converging biocrust development and increasing diversity encourages establishment of interdependent microbial interactions

Biocrusts are multispecies assemblies that maximize diversity (Chilton et al. 2018). Highly diverse biocrust communities have been associated with functional redundancy (Li et al. 2020, Baumann et al. 2021, Miralles et al. 2021) and symbioses (Nelson et al. 2021). As cooperative microbial interactions are often more energetically efficient than individual efforts (Freilich et al. 2011, Machado et al. 2021), these communities could conceivably use resources more effectively than their extremophile counterparts. In the adverse conditions of harsh environments such as highly saline potash heaps, biocrusts can also provide safe spaces away from direct grazing with the contribution of soil particle cementing EPS. In this study, prokaryotic diversity increased along both transects, as hypothesized. Maier et al. (2018) similarly found clear shifts in heterotrophic communities, with an increase in bacterial and fungal alpha diversity with biocrust succession, but observed a shift from generalists to specialists, in opposition to this study. On the other hand, Xu et al. (2020) observed a decrease in diversity upon succession (opposing our study) in desert biocrusts and a shift from specialists to generalists along a successional gradient (in agreement with our study). As such, we agree with Read et al. (2016), who proposed alternate models for succession should be used in 'favourable' and 'unfavourable' conditions.

In this study, analyses with phylogenetically informed UniFrac distances revealed that the microbiomes converged along the successional gradients and became more similar to each other, which was not obvious by using only hierarchical clustering methods. Similarly, Xu et al. (2020), also found that biocrusts in the Gurbantunggut desert in Northwestern China converged, and that an increase of generalists drove this convergence. Moreover, this is in line with the Anna Karenina Hypothesis, which states 'all happy families are alike (healthy microbiomes) but unhappy families (dysbiosis) are different' (Zaneveld et al. 2017, Ma 2020). We could argue that biocrust microbiomes are 'happy families' that are more resistant to stressors, and highly specialized saline heap microbiomes are 'unhappy', and thus more phylogenetically distant due to their unfavourable conditions. Moreover, Cyanobacterial dominance in the initial stages of biocrust formation may have initiated more complex community establishment that guided this microbiome convergence.

Physically, interwoven cyanobacterial filaments form microspaces that can act as protective regions (Dawidowicz 1990, Day et al. 2017), and create more surface area. Further, biofilms formed by the EPS matrix improve nutrient exchange and interspecies communication and interaction. Biochemically, heterocystous Cyanobacteria form strong symbioses, such as a C for N exchange with bacterial heterotrophs when N is scarce in desert biocrusts (Nelson et al. 2021). Considering Cyanobacteria were site-specific, higher concentrations of TDN at the WT site may be attributable to N<sub>2</sub> fixation, potentially by diazotrophs in the cyanosphere (Nelson et al. 2021) that were only found in the WT initial and biocrust stages, but not in OD as previously reported by direct microscopy and a culture approach (Sommer et al. 2020a). In addition, the N2-fixing Nostoc only found at the WT site and not at the OD site (Sommer et al. 2020a) could have contributed to

Additionally, we found biocrust-associated genera such as Burkholderia and Pseudoxanthomonas, which are known for phosphate solubilization, EPS-production, and siderophore production ability (Nelson et al. 2021), and cellulose and chitin degraders such as Chthoniobacter, likely involved in organic C breakdown (Chirak et al. 2017). Superphylum Patescibacteria, a recently discovered clade whose members are known for reduced genomes, and thus implicated in obligate symbioses (Nelson and Stegen 2015, Tian et al. 2020) increased along the transects. We also found Pseudonocardia, an acinomycete known to produce antifungals, antimicrobials, and secondary metabolites implicated in bioremediation (Riahi et al. 2022). It increased along the transects, potentially serving as a protectant against pathogen invasion into the biocrust communities, echoing the symbiotic relationship documented between the bacteria and leaf cutter ants (Goldstein and Klassen 2020).

We demonstrate the development from an 'uninhabitable', low diversity environment largely populated by specially adapted extremophiles to a more dynamic, robust environment. The abiotic and biotic properties of this environmental conversion inherently make more resources available for and provide niches to generalists, and potentially allow for more complex relationships such as competition and interdependent interactions.

# Biocrust establishment is associated with phylogenetic turnover, as community assembly transitions from stochastic to deterministic

We found the majority (60%-73%) of community assembly in our biocrusts was directed by variable selection (deterministic), indicating more than expected phylogenetic turnover. Others found desert biocrusts were driven by dispersal limitation (stochastic) (Li and Hu 2021), or homogenous selection (deterministic) (Xu et al. 2020), and that the balance between stochastic and deterministic processes was mediated by abiotic metrics such as salinity (Li and Hu 2021). Further, in the above mentioned study from the Gurbantunggut desert, total organic C/N ratio and pH were key drivers of community assembly (Xu et al. 2021). In our study, a significant portion of the biocrust stage at the WT site (~ 20%) were also assembled with homogenizing selection, indicating less than expected phylogenetic turnover. As such, we propose some species were already adapted (did not turn over) in the WT as compared to OD. In contrast, Euryarchaeota made up a large portion (> 50%) of the heap bacterial communities at the OD site, and the disappearance of this archaeal kingdom following biocrust development could indicate more 'turnover' in the OD than in the WT.

We must note that our assessment of community assembly processes did not consistently align with a comparable method, iCAMP, which indicated a higher proportion of stochastic processes (data not shown). Consequently, our analysis may have overestimated the role of deterministic processes. However, iCAMP has limitations with diversification, competition, and can underestimate selection in certain scenarios (Ning et al. 2020). Considering that this is an examination of biocrusts, which are intimately entwined communities where symbiotic nutrient exchange and competition for niche space occurs as they develop, and that all other findings suggested microbiome convergence, we accept that the decision to use beta-NTI was reasonable in this case

#### **Conclusions**

We showed heap to biocrust succession is site-specific, yet consistent in its progression. Succession increases niche space through abiotic and biotic means, and recruits a diverse array of taxa into an interdependent meta-community. This could provide a more attractive, nutrient rich environment for higher-level plants normally unsuited to bare salt heap environments. In degraded systems such as potash salt heaps, Cyanobacteria act as ecosystem engineers and therefore catalysts for biocrust formation, lowering the 'activation energy' needed to establish a more diverse and interconnected microbiome. This can improve the chances for higher kingdom colonization by increasing mutualistic interactions. However, considering this was an observational field study, we cannot say for sure if the observed microbial succession resulted from changing abiotic factors such as decreased salinity, and/or if the biocrusts themselves changed the environment. Likely there was some threshold at which colonization and subsequent succession were possible, which led to a positive feedback loop of nutrient input and cycling. Our work provides context into the microbial composition and succession of naturally

occurring biocrusts in extreme regions and the driving forces behind their community assembly. Though we can only speak for potash salt heaps, future studies would compare the microbiome succession of biocrusts in other biomes and degraded areas, and determine key drivers of community assembly. Future work would also disentangle abiotic factors such as differing seasonal dynamics, which could inform developmental stages. Further, the specific identification of important biocrust relationship types, such as the C for N exchange between Cyanobacteria and heterotrophs, as well as the role of other important microbiota such as fungi, would be essential in aiding in solutions targeted toward biocrust establishment and resilience in order to restore degraded environments and combat the effects of climate change.

### **Author contributions**

Juliette A. Ohan (Data curation, Formal analysis, Investigation, Visualization, Writing - original draft, Writing - review & editing), Roberto Siani (Data curation, Formal analysis, Visualization, Writing - review & editing), Julia K. Kurth (Resources, Writing - review & editing), Veronika Sommer (Investigation, Resources, Writing review & editing), Karin Glaser (Resources), Ulf Karsten (Conceptualization, Funding acquisition, Supervision, Writing - review & editing), Michael Schloter (Conceptualization, Supervision, Writing - review & editing), and Stefanie Schulz (Conceptualization, Supervision, Writing – review & editing)

# **Acknowledgements**

Many thanks to the Nature Conservation Authority of the Peine and Lüchow-Dannenberg districts, as well as the Wietze community, the GESA (Gesellschaft zur Entwicklung und Sanierung von Altstandorten MBH), and PD Dr Albrecht Palm for granting permission and/or access to the sampling sites.

# Supplementary data

Supplementary data are available at FEMSEC Journal online.

Conflict of interest. The authors declare that they have no commercial or financial conflict of interest.

# **Funding**

This project was funded by the Deutsche Bundesstiftung Umwelt (DBU) and the Gesellschaft für Chemische Technik und Biotechnologie e.V. (DECHEMA), Max-Buchner-Forschungsstipendium (MBFSt 3583).

# Data availability

The 16S rRNA gene amplicon sequences were submitted to the NCBI sequencing read archive under Bioproject ID PRJNA934864.

#### References

Abed RMM, Tamm A, Hassenrück C et al. Habitat-dependent composition of bacterial and fungal communities in biological soil crusts from Oman. Sci Rep 2019;9:6468.

Andersen KS, Kirkegaard RH, Karst SM et al. ampvis2: an R package to analyse and visualise 16S rRNA amplicon data. Biorxiv 2018; https://doi.org/10.1101/299537

- Apprill A, McNally S, Parsons R et al. Minor revision to V4 region SSU rRNA 806R gene primer greatly increases detection of SAR11 bacterioplankton. Aquat Microb Ecol 2015;75:129-37.
- Averill C, Werbin ZR, Atherton KF et al. Soil microbiome predictability increases with spatial and taxonomic scale. Nat Ecol Evol 2021;**5**:747-56.
- Bach H-J, Tomanova J, Schloter M et al. Enumeration of total bacteria and bacteria with genes for proteolytic activity in pure cultures and in environmental samples by quantitative PCR mediated amplification. J Microbiol Methods 2002;49: 235-45
- Balázs HE, Schmid CA, Cruzeiro C et al. Post-reclamation microbial diversity and functions in hexachlorocyclohexane (HCH) contaminated soil in relation to spontaneous HCH tolerant vegetation. Sci Total Environ 2021;767:144653.
- Bano N, Ruffin S, Ransom B et al. Phylogenetic composition of Arctic Ocean archaeal assemblages and comparison with Antarctic assemblages. Appl Environ Microbiol 2004;70:781-9.
- Barnett SE, Youngblut ND, Buckley DH. Soil characteristics and landuse drive bacterial community assembly patterns. FEMS Microbiol Ecol 2020:96:fiz194.
- Battista JR Against all odds: the survival strategies of Deinococcus radiodurans. Annu Rev Microbiol 1997;51:203-24.
- Baumann K, Eckhardt K-U, Acksel A et al. Contribution of biological soil crusts to soil organic matter composition and stability in temperate forests. Soil Biol Biochem 2021;160:108315.
- Belnap J, Büdel B, Lange OL. Biological soil crusts: characteristics and distribution. In: Biological Soil Crusts: Structure, Function, and Management, Berlin: Springer, 2001,3-30.
- Belnap J. Biological phosphorus cycling in dryland regions. In: Phosphorus in Action, Berlin: Springer, 2011,371-406.
- Belnap J. The potential roles of biological soil crusts in dryland hydrologic cycles. Hydrol Process 2006;20:3159-78.
- Benjamini Y, Hochberg Y. Controlling the false discovery rate: a practical and powerful approach to multiple testing. J R Stat Soc Ser B Stat Methodol 1995;57:289-300.
- Beule L, Karlovsky P. Improved normalization of species count data in ecology by scaling with ranked subsampling (SRS): application to microbial communities. PeerJ 2020;8:e9593.
- Bolyen E, Rideout JR, Dillon MR et al. Reproducible, interactive, scalable, and extensible microbiome data science using QIIME 2. Nat Biotechnol 2018;37:852-7.
- Bowker MA, Belnap J, Büdel B et al. Controls on distribution patterns of biological soil crusts at micro-to global scales. In: Biological Soil Crusts: An Organizing Principle in Drylands, Berlin: Springer, 2016, 173-97.
- Callahan BJ, McMurdie PJ, Rosen MJ et al. DADA2: high-resolution sample inference from Illumina amplicon data. Nat Methods 2016;**13**:581-3.
- Cania B, Vestergaard G, Kublik S et al. Biological soil crusts from different soil substrates harbor distinct bacterial groups with the potential to produce exopolysaccharides and lipopolysaccharides. Microb Ecol 2020;79:326-41.
- Carreto L, Moore E, Nobre MF et al. Rubrobacter xylanophilus sp. nov., a new thermophilic species isolated from a thermally polluted effluent. Int J Syst Evol Microbiol 1996;46:460-5.
- Chamizo S, Cantón Y, Miralles I et al. Biological soil crust development affects physicochemical characteristics of soil surface in semiarid ecosystems. Soil Biol Biochem 2012;49:96-105.
- Chamizo S, Cantón Y, Rodríguez-Caballero E et al. Biocrusts positively affect the soil water balance in semiarid ecosystems. Ecohydrol 2016;**9**:1208-21.

- Chamizo S, Rodríguez-Caballero E, Román JR et al. Effects of biocrust on soil erosion and organic carbon losses under natural rainfall. Catena 2017;148:117-25.
- Chase JM, Kraft NJ, Smith KG et al. Using null models to disentangle variation in community dissimilarity from variation in  $\alpha$ -diversity. Ecosphere 2011;**2**:1–11.
- Chase JM, Myers JA. Disentangling the importance of ecological niches from stochastic processes across scales. Phil Trans R Soc B 2011;**366**:2351-63.
- Chilton AM, Neilan BA, Eldridge DJ. Biocrust morphology is linked to marked differences in microbial community composition. Plant Soil 2018;429:65-75.
- Chirak E, Orlova O, Aksenova T et al. Dynamics of chernozem microbial community during biodegradation of cellulose and barley straw. Agric Biol 2017;52:588-96.
- Cowles HC. The ecological relations of the vegetation on the sand dunes of Lake Michigan. Part I. - geographical relations of the dune floras. Botan Gazette 1899;27:95-117.
- Davis NM, Proctor DM, Holmes SP et al. Simple statistical identification and removal of contaminant sequences in marker-gene and metagenomics data. Microbiome 2018;6:1-14.
- Dawidowicz P. The effect of Daphnia on filament length of blue-green algae. Hydrobiologia 1990;191:265-8.
- Day JG, Gong Y, Hu Q. Microzooplanktonic grazers-a potentially devastating threat to the commercial success of microalgal mass culture. Algal Res 2017;27:356-65.
- Deutscher Wetterdienst. Klimaatlas Deutschland: Klimamittel, State: Lower Saxony (Niedersachsen), Location: Celle (#850); Braunschweig (# 662), Period: 1991-2020. 2023a. https://opendata. dwd.de/climate\_environment/CDC/observations\_germany/ climate/multi\_annual/mean\_91-20/Temperatur\_1991-2020.txt (2 May 2023, date last accessed).
- Deutscher Wetterdienst. Klimaatlas Deutschland: Klimamittel, State: Lower Saxony (Niedersachsen), Location: Celle (#850); Braunschweig (# 662), Period: 1991-2020. 2023b. https://opendata. dwd.de/climate\_environment/CDC/observations\_germany/ climate/multi\_annual/mean\_91-20/Niederschlag\_1991-2020.txt (2 May 2023, date last accessed).
- Dixon P. VEGAN, a package of R functions for community ecology. J Veg Sci 2003;14:927-30.
- Drahorad SL, Felde VJ, Ellerbrock RH et al. Water repellency decreases with increasing carbonate content and pH for different biocrust types on sand dunes. J Hydrol Hydromech 2021;69: 369-77
- Fierer N, Jackson RB. The diversity and biogeography of soil bacterial communities. Proc Natl Acad Sci USA 2006;103:626-31.
- Fierer N, Nemergut D, Knight R et al. Changes through time: integrating microorganisms into the study of succession. Res Microbiol 2010;161:635-42.
- Freilich S, Zarecki R, Eilam O et al. Competitive and cooperative metabolic interactions in bacterial communities. Nat Commun 2011:2:589.
- Gall C, Ohan J, Glaser K et al. Biocrusts: overlooked hotspots of managed soils in mesic environments. J Plant Nutr Soil Sci 2022;**185**:745-51.
- Garcia-Pichel F, Belnap J. Microenvironments and microscale productivity of cyanobacterial desert crusts. J Phycol 1996;32:774-82.
- Garve E, Garve V. Halophytes at potash mine dumps in Germany and France (Alsace). Tuexenia 2000;20:375-417.
- Glaser K, Albrecht M, Baumann K et al. Biological soil crust from mesic forests promote a specific bacteria community. Front Microbiol 2022;13:769767.

- Goldstein SL, Klassen JL. Pseudonocardia symbionts of fungusgrowing ants and the evolution of defensive secondary metabolism. Front Microbiol 2020;11:621041.
- Gypser S, Veste M, Fischer T et al. Infiltration and water retention of biological soil crusts on reclaimed soils of former open-cast lignite mining sites in Brandenburg, north-east Germany. J Hydrol Hydromech 2016;64:1.
- Ihaka R, Gentleman R. R: a language for data analysis and graphics. J Comput Graph Stat 1996;5:299-314.
- Kamilar JM, Cooper N. Phylogenetic signal in primate behaviour, ecology and life history. Phil Trans R Soc B 2013;368:20120341.
- Kolde R, Kolde MR. Package 'pheatmap'. R Package 2015;1:790.
- Könneke M, Bernhard AE, de L et al. Isolation of an autotrophic ammonia-oxidizing marine archaeon. Nature 2005;437:543-6.
- Kuhn M. Building predictive models in R using the caret package. J Stat Soft 2008;28:1-26.
- Kurth JK, Albrecht M, Karsten U et al. Correlation of the abundance of bacteria catalyzing phosphorus and nitrogen turnover in biological soil crusts of temperate forests of Germany. Biol Fertil Soils 2021:57:179-92.
- Lahti L, Shetty S. Introduction to the microbiome R package. GitHub, Inc. 2018.
- Lauber CL, Hamady M, Knight R et al. Pyrosequencing-based assessment of soil pH as a predictor of soil bacterial community structure at the continental scale. Appl Environ Microbiol 2009;75: 5111-20
- Le Provost G, Schenk NV, Penone C et al. The supply of multiple ecosystem services requires biodiversity across spatial scales. Nat Eco Euol 2023;7:236-49.
- Lee KC, Caruso T, Archer SD et al. Stochastic and deterministic effects of a moisture gradient on soil microbial communities in the McMurdo Dry Valleys of Antarctica. Front Microbiol 2018;9:
- Li H, Huo D, Wang W et al. Multifunctionality of biocrusts is positively predicted by network topologies consistent with interspecies facilitation. Mol Ecol 2020;29:1560-73.
- Li Y, Hu C. Biogeographical patterns and mechanisms of microbial community assembly that underlie successional biocrusts across northern China. Npj Biofilms Microbiomes 2021;7: 1-11.
- Liu N, Hu H, Ma W et al. Relative importance of deterministic and stochastic processes on soil microbial community assembly in temperate grasslands. Microorganisms 2021;9:1929.
- McMurdie PJ, Holmes S. phyloseg: an R package for reproducible interactive analysis and graphics of microbiome census data. PLoS ONE 2013;8:e61217.
- Ma ZS. Testing the Anna Karenina principle in human microbiomeassociated diseases. iScience 2020;23:101007.
- Machado D, Maistrenko OM, Andrejev S et al. Polarization of microbial communities between competitive and cooperative metabolism. Nat Ecol Evol 2021;5:195-203.
- Maier S, Tamm A, Wu D et al. Photoautotrophic organisms control microbial abundance, diversity, and physiology in different types of biological soil crusts. ISME J 2018;12:1032-46.
- Miralles I, Ortega R, Montero-Calasanz MC. Studying the microbiome of cyanobacterial biocrusts from drylands and its functional influence on biogeochemical cycles. Res Square Prepr 2021. https://doi.org/10.21203/rs.3.rs-252045/v1
- Nelson C, Giraldo-Silva A, Garcia-Pichel F. A symbiotic nutrient exchange within the cyanosphere microbiome of the biocrust cyanobacterium, Microcoleus vaginatus. ISME J 2021;15: 282-92.

- Nelson WC, Stegen JC. The reduced genomes of Parcubacteria (OD1) contain signatures of a symbiotic lifestyle. Front Microbiol
- Nicol GW, Glover LA, Prosser JI. Spatial analysis of archaeal community structure in grassland soil. Appl Environ Microbiol 2003;69:7420-9.
- Ning D, Yuan M, Wu L et al. A quantitative framework reveals ecological drivers of grassland microbial community assembly in response to warming. Nat Commun 2020;11:4717.
- Norman JS, King GM, Friesen ML. Rubrobacter spartanus sp. nov., a moderately thermophilic oligotrophic bacterium isolated from volcanic soil. Int J Syst Evol Microbiol 2017;67:3597-602.
- Parada AE, Needham DM, Fuhrman JA. Every base matters: assessing small subunit rRNA primers for marine microbiomes with mock communities, time series and global field samples. Environ Microbiol 2016:18:1403-14.
- Pushkareva E, Sommer V, Barrantes I et al. Diversity of microorganisms in biocrusts surrounding highly saline potash tailing piles in Germany. Microorganisms 2021;9:714.
- Quast C, Pruesse E, Yilmaz P et al. The SILVA ribosomal RNA gene database project: improved data processing and web-based tools. Nucleic Acids Res 2012;41:D590-6.
- Rainey FA, Ray K, Ferreira M et al. Extensive diversity of ionizingradiation-resistant bacteria recovered from Sonoran Desert soil and description of nine new species of the genus Deinococcus obtained from a single soil sample. Appl Environ Microbiol 2005;71:5225-35.
- Rath KM, Fierer N, Murphy DV et al. Linking bacterial community composition to soil salinity along environmental gradients. ISME J 2019;13:836-46.
- Raup DM, Crick RE. Measurement of faunal similarity in paleontology. J Palentol 1979;53:1213-27.
- Read CF, Elith J, Vesk PA. Testing a model of biological soil crust succession. J Veg Sci 2016;27:176-86.
- Riahi HS, Heidarieh P, Fatahi-Bafghi M. Genus Pseudonocardia: what we know about its biological properties, abilities and current application in biotechnology. J Appl Microbiol 2022;132:890-906.
- Ritchie R. Universal chlorophyll equations for estimating chlorophylls a, b, c, and d and total chlorophylls in natural assemblages of photosynthetic organisms using acetone, methanol, or ethanol solvents. Photosynt 2008;46:115-26.
- Rivera-Aguilar V, Godínez-Alvarez H, Moreno-Torres R et al. Soil physico-chemical properties affecting the distribution of biological soil crusts along an environmental transect at Zapotitlán drylands, Mexico. J Arid Environ 2009;73:1023-8.
- Riveras-Muñoz N, Seitz S, Witzgall K et al. Biocrust-linked changes in soil aggregate stability along a climatic gradient in the Chilean Coastal Range. SOIL 2022;8:1-28.
- Rossi F, Mugnai G, De Philippis R. Cyanobacterial biocrust induction: a comprehensive review on a soil rehabilitation-effective biotechnology. Geoderma 2022;415:115766.
- Schliep KP. phangorn: phylogenetic analysis in R. Bioinformatics 2011;27:592-3.
- Schöler A, Jacquiod S, Vestergaard G et al. Analysis of soil microbial communities based on amplicon sequencing of marker genes. Biol Fert Soils 2017;53:485-9.
- Schöps R, Goldmann K, Herz K et al. Land-use intensity rather than plant functional identity shapes bacterial and fungal rhizosphere communities. Front Microbiol 2018;9:2711.
- Sommer V, Karsten U, Glaser K. Halophilic algal communities in biological soil crusts isolated from potash tailings pile areas. Front Ecol Evol 2020a;8. https://doi.org/10.3389/fevo.2020.00046

- Sommer V, Mikhailyuk T, Glaser K et al. Uncovering unique green algae and cyanobacteria isolated from biocrusts in highly saline potash tailing pile habitats, using an integrative approach. Microorganisms 2020b;8:1667.
- Stegen JC, Lin X, Fredrickson JK et al. Quantifying community assembly processes and identifying features that impose them. ISME J 2013;7:2069–79.
- Stegen JC, Lin X, Konopka AE et al. Stochastic and deterministic assembly processes in subsurface microbial communities. ISME J 2012;6:1653–64.
- Su Y-g, Zhao X, Li A-x et al. Nitrogen fixation in biological soil crusts from the Tengger desert, northern China. Eur J Soil Biol 2011;47:182–7.
- Sun F, Xiao B, Li S et al. Towards moss biocrust effects on surface soil water holding capacity: soil water retention curve analysis and modeling. *Geoderma* 2021;**399**:115120.
- Thiet RK, Boerner REJ, Nagy M et al. The effect of biological soil crusts on throughput of rainwater and n into Lake Michigan sand dune soils. Plant Soil 2005;278:235–51.
- Tian R, Ning D, He Z et al. Small and mighty: adaptation of superphylum Patescibacteria to groundwater environment drives their genome simplicity. Microbiome 2020;8:1–15.
- Töwe S, Wallisch S, Bannert A et al. Improved protocol for the simultaneous extraction and column-based separation of DNA and RNA from different soils. J Microbiol Methods 2011;84: 406–12.
- Treusch AH, Leininger S, Kletzin A et al. Novel genes for nitrite reductase and Amo-related proteins indicate a role of uncultivated mesophilic crenarchaeota in nitrogen cycling. Environ Microbiol 2005;7:1985–95.

- Tripathi BM, Stegen JC, Kim M et al. Soil pH mediates the balance between stochastic and deterministic assembly of bacteria. ISME J 2018;12:1072–83.
- Wang J, Shen J, Wu Y et al. Phylogenetic beta diversity in bacterial assemblages across ecosystems: deterministic versus stochastic processes. ISME J 2013;7:1310–21.
- Wasimuddin, Schlaeppi K, Ronchi F et al. Evaluation of primer pairs for microbiome profiling from soils to humans within the One Health framework. Mol Ecol Resour 2020;20:1558–71.
- Wickham H. ggplot2. WIREs Comp Stat 2011;3:180-5.
- Wright ES, Yilmaz LS, Noguera DR. DECIPHER, a search-based approach to chimera identification for 16S rRNA sequences. Appl Environ Microbiol 2012;78:717–25.
- Xiao B, Sun F, Hu K et al. Biocrusts reduce surface soil infiltrability and impede soil water infiltration under tension and ponding conditions in dryland ecosystem. J Hydrol 2019;568:792–802.
- Xu L, Zhang B, Wang E et al. Soil total organic carbon/total nitrogen ratio as a key driver deterministically shapes diazotrophic community assemblages during the succession of biological soil crusts. Soil Ecol Lett 2021;3:328–41.
- Xu L, Zhu B, Li C et al. Development of biological soil crust prompts convergent succession of prokaryotic communities. *Catena* 2020;**187**:104360.
- Zaneveld JR, McMinds R, Vega Thurber R. Stress and stability: applying the Anna Karenina principle to animal microbiomes. *Nat Microbiol* 2017;**2**:1–8.
- Zhang Y, Wang H, Wang X et al. The microstructure of microbiotic crust and its influence on wind erosion for a sandy soil surface in the Gurbantunggut Desert of Northwestern China. *Geoderma* 2006;**132**:441–9